Nanopatterning of Cu-Ligated Mercaptoalkanoic Acid Multilayers on Si Substrates via Atomic Force Lithography

Alexandra M. Patron[1], Alisha M. Bramer[2], Daniel F. Santavicca[2], and Thomas J. Mullen[1*]

November 4, 2019

[1]Department of Chemistry, University of North Florida, Jacksonville, FL 32224 USA

[2]Department of Physics, University of North Florida, Jacksonville, FL 32224 USA

[*]Corresponding author's email: tj.mullen@unf.edu

ABSTRACT

Chemical self-assembly has garnered tremendous interest as a tool for generating nanometer-scale structures and devices. Organosilane self-assembled monolayers (SAMs) are of particular interest due to their ability to assemble on a wide range of substrates with varied chemical functionalities. Nanoshaving, an atomic force lithographic technique, has been demonstrated as a method to generate nanopatterns of organosilane SAMs. However, this method requires extremely high force setpoints, which rapidly dulls atomic force microscopy tips and degrades the resolution of the resulting nanopattern. In this work, we utilize Cu-ligated mercaptohexadecanoic acid (MHDA) multilayers to circumvent this limitation. Initially, a 10-undecenyltrichlorosilane (UTS) SAM is assembled onto a Si substrate, and the terminal olefin groups of the UTS SAM are oxidized to carboxyl groups. Subsequently, a Cu-ligated MHDA multilayer is assembled via the sequential deposition of Cu^{2+} ions and MHDA molecules. The interface between the oxidized UTS SAM and Cu-ligated MHDA multilayer serves as a natural low force breakpoint for nanoshaving. We demonstrate that the resulting nanopatterns can function as a chemical resist to fabricate metal nanostructures.

INTRODUCTION

Organosilane self-assembled monolayers (SAMs) have been employed as versatile molecular architectures for electronic, optical, and sensing platforms.[1-4] Interest in these SAMs stems from the broad range of chemical functionalities and the ability to assemble them on various substrates including semiconductor oxides, metal oxides, glass, mica, and quartz.[5-12] A number of strategies have been devised to pattern organosilane SAMs including photolithography, electron-beam lithography, contact-printing lithography, particle lithography, and scanning probe lithography.[13-23]

Nanoshaving, a type of scanning probe lithography, generates chemical patterns by moving an atomic force microscopy (AFM) tip in a predetermined track at a high force setpoint to induce desorption within a chemical film.[24-25] This *in-situ* technique enables real-time characterization (at lower force setpoints) in order to locate an appropriate region for patterning. Once a pattering step is completed, the resulting chemical structure can be characterized before moving on to the next pattering step. While nanoshaving is a serial technique, it has the potential be combined with parallel patterning techniques such as photolithography. In such a hybrid approach, larger wafer-scale features could be patterned with photolithography, and, subsequently, nanoscale features could be defined via nanoshaving with nanoscale alignment to the large-scale features.

One of the challenges of nanoshaving organosilane SAMs is that the force setpoints required for tip-induced desorption are very large (~μN) as a result of breaking the Si-O bonds at the organosilane-oxide interface.[26-28] A consequence of these large forces is that AFM tips rapidly

dull, which degrades the patterning and imaging resolution. This can also lead to incomplete desorption of the organosilane SAM.

In this report, we explore the use of Cu-ligated MHDA multilayers to circumvent the limitations of nanoshaving organosilane SAMs. These multilayers are assembled by depositing sequential alternating layers of MHDA molecules and cupric ions (Cu^{2+}) across the sample.[29-33] Cu-ligated MHDA multilayers have previously been used as "molecular rulers" to build up precise nanoscale lithographic resists that can define spaces between metal features.[34] Cu-ligated MHDA multilayers can be patterned easily by nanoshaving because they require relatively low force setpoints (~40 nN).[30] However, these Cu-ligated MHDA multilayers are usually only assembled on Au substrates.[29, 31-32, 35] We extend this approach to other substrates by depositing a 10-undecenyltrichlorosilane (UTS) SAM and oxidizing the terminal olefin groups to carboxyl functionalities (UTS_{ox}). The carboxyl groups enable the Cu-ligated MHDA multilayer to be assembled onto the preexisting organosilane SAM. The interface between the UTS_{ox} SAM and the Cu-ligated MHDA multilayer provides a breakpoint for nanoshaving at low force setpoints. This enables the use of nanoshaving to create chemical patterns on a wide range of substrates that can then serve as lithographic resists for metal deposition.

EXPERIMENTAL

Materials and Reagents

Boron-doped, polished Si(111) substrates were purchased from Ted Pella (Redding, CA). These substrates were precut to lateral dimensions of 10 mm × 10 mm. Toluene (ACS Grade), bicyclohexyl (>99.0%), hydrogen peroxide (30% aqueous solution), sulfuric acid (ACS Grade),

ammonium hydroxide (ACS Grade), sodium periodate (99%), potassium carbonate (anhydrous, ACS Grade), and potassium permanganate (99+%) were purchased from VWR International (Randor, PA). 16-mercaptohexadecanoic acid (MHDA, 90%) and copper (II) perchlorate hexahydrate ($Cu(ClO_4)_2 \cdot 6H_2O$, 98%) were purchased from Sigma Aldrich (St. Louis, MO). 10-undecenyltrichlorosilane (UTS) was purchased from Gelest (Morrisville, PA). Absolute ethanol was purchased from Pharmco-Aaper (Bookfield, CT). Au (99.999%) and Cr (99.95%) pellets were purchased from Kurt J. Lesker Company (Pittsburg, PA). ACT-935 was purchased from Air Products (Allentown, PA). All reagents were used as received. Water (18 MΩ) was generated using a Milli-Q system (Q-GARD 2, Millipore, Billerica, MA). All glassware was cleaned by immersing in piranha solution (3:1 by volume of sulfuric acid/30% hydrogen peroxide) for 1 h, rinsing with copious amounts of 18 MΩ water, and drying overnight in ambient. *Caution: piranha is a vigorous oxidant and should be used with extreme care!*

Preparation of Si Substrates

Si substrates were cleaned by immersing in piranha solution (3:1 by volume of sulfuric acid/30% hydrogen peroxide) for 1 h, rinsing with copious amounts of 18 MΩ water, submersing in a base etch solution (5:1:1 by volume of 18 MΩ water/ammonium hydroxide/30% hydrogen peroxide) with heating in an oven at 75°C for 1 h, rinsing with copious amounts of 18 MΩ water, immersing in piranha solution (3:1 by volume of sulfuric acid/30% hydrogen peroxide) for 1 h, and finally rinsing with copious amounts of 18 MΩ water. The Si substrates were stored in 18 MΩ water prior to use for at most 48 hours. The Si substrates were dried under a stream of N_2 prior to use in multilayer assembly.

Preparation Cu-Ligated MHDA Multilayers on Si Substrates

Cu-ligated MHDA multilayers on Si substrates were fabricated using the strategy depicted in Figure 1. UTS monolayers were prepared by immersing Si substrates into 5 mM bicyclohexyl solutions of UTS overnight (18-24 h). The Si substrates were then rinsed with toluene, dried under stream of N_2, rinsed with ethanol, and dried again under a stream of N_2. Subsequently, the terminal olefin groups of the UTS molecules were oxidized to carboxyl groups using previously described methods.[9, 22] Briefly, 1 mL aliquots of stock solutions of $KMnO_4$ (5 mM), KIO_4 (200 mM), and K_2CO_3 (20 mM) were mixed with 7 mL of 18 MΩ water. The Si substrates with the UTS monolayers were immersed into these freshly-prepared aqueous solutions overnight (18-24 h). The Si substrates were sequentially rinsed with copious amounts of 18 MΩ water, 0.3 M $NaHSO_3$, 18 MΩ water, 0.1 N HCl, 18 MΩ water, and ethanol and then dried under a stream of N_2. To assemble the Cu-ligated MHDA multilayers, the Si substrates were immersed into 0.1 mM $Cu(ClO_4)_2 \cdot 6H_2O$ ethanolic solutions for 3 min, rinsed with ethanol, immersed into 0.1 mM MHDA ethanolic solutions for 10 min, and rinsed with ethanol. This sequence of immersion into ethanolic solutions of $Cu(ClO_4)_2 \cdot 6H_2O$ and MHDA was repeated until the number of desired layers was achieved using a custom-built sample dipper based on an OpenBuilds ACRO positioning system (Monroeville, NJ). To deposit metal onto the Cu-ligated MHDA multilayers, the Si substrates were placed into a custom-built thermal deposition system. After reaching a pressure of $<10^{-6}$ Torr, 3 nm of Cr was deposited at a rate of 0.2 Å/s as an adhesion layer, followed by the deposition of 10 nm of Au at a rate of 1.2 Å/s. To remove the Cu-ligated MHDA multilayers, the Si substrates were soaked in ACT-935 at 75 °C for 1 h followed by sonication for 5 min. The substrates were then rinsed in ethanol and dried under a stream of N_2.

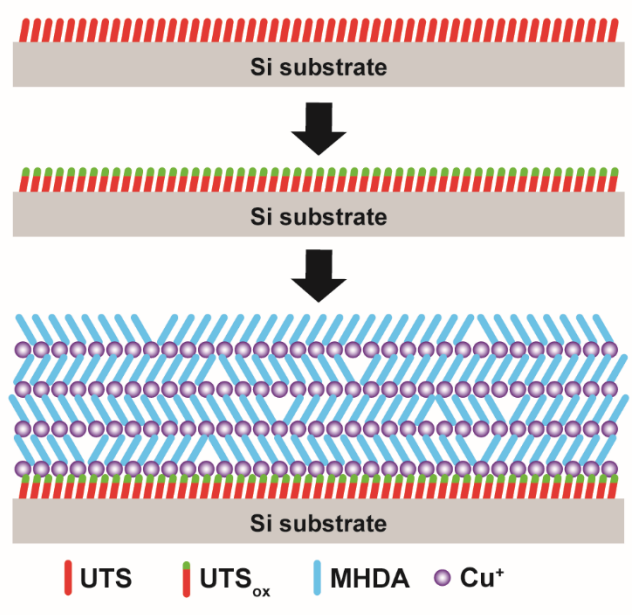

Figure 1. Key steps for the assembly of Cu-ligated MHDA multilayer on Si substrates. A UTS SAM is fabricated on a Si substrate via immersion into a 5 mM bicyclohexyl solution of UTS overnight. The terminal olefin groups of the UTS molecule are oxidized to carboxyl groups via immersion into a $KMnO_4$, KIO_4, and K_2CO_3 solution overnight. The Cu-ligated MHDA multilayer is assembled via sequential immersion into 0.1 mM $Cu(ClO_4)_2 \cdot 6H_2O$ ethanolic solutions for 3 min and into 0.1 mM MHDA ethanolic solutions for 10 min until the number of desired layers is achieved.

Atomic Force Microscopy

Contact-mode AFM images were acquired using an Agilent 5420 Scanning Probe Microscope with sharpened Si_3N_4 cantilevers (DNP-S, Bruker AFM Probes, Santa Barbra, CA) with nominal force constants of 0.35 N/m. Force constants for individual cantilevers were measured via the thermal noise method and ranged from 0.25 N/m to 0.50 N/m.[36] The Si_3N_4 cantilevers were cleaned using a UV ozone cleaner (Novascan, PSDP-UVT, Ames, IA) for 20 min to remove

surface contaminants.[37] Imaging force setpoints at or below 1 nN were utilized to minimize damage to and disruption of the UTS monolayers and Cu-ligated MHDA multilayers, and scan rates were set to 1 Hz to maximize topographic tracking. All AFM images were acquired at 256 points per line. Image processing and analysis of the AFM images were performed using Gwyddion (version 2.54, "A Small Step"), which is an open-source software freely available on the internet and supported by the Czech Metrology Institute. [38]

Nanoshaving

Nanoshaving is an *in-situ* AFM-based lithographic technique developed by Liu and coworkers to expose underlying regions within chemical films.[24-25] Chemical patterns are generated by moving an AFM tip in predetermined track at a high force setpoint (30-1000 nN) to induce desorption within a chemical film. In a typical nanoshaving experiment for this study, a Si substrate with a Cu-ligated MHDA multilayer assembled on a preexisting UTS_{ox} SAM was imaged at low force setpoint (~1 nN) under ethanol to characterize the substrate and to locate an appropriate region for patterning. Using a high force setpoint (30-100 nN, depending on the sharpness of the AFM tip), the oxidized UTS (UTS_{ox}) monolayer was exposed due to the tip-induced desorption of the Cu-ligated MHDA multilayer. Subsequently, the patterned region was imaged at a low force setpoint (~1 nN) to characterize the resulting chemical patterning. The force setpoints for imaging and nanoshaving were quantified by using force-distance curves before each imaging and nanoshaving step. The force setpoints for nanoshaving were determined by systematically increasing the force setpoint until selective desorption of the Cu-ligated MHDA multilayer was observed.[39-40] All nanoshaved regions were generated at 512

points per line and under absolute ethanol to minimize surface contamination and to promote nanoshaving.

Determining RMS Roughnesses and Apparent Heights of UTS Monolayers, UTS_{ox} Monolayers, and Cu-Ligated MHDA Multilayers.

The RMS roughnesses for the UTS monolayers, UTS_{ox} monolayers, and Cu-ligated MHDA multilayers were calculated using a set of at least four 2 μm × 2 μm AFM images for each type of chemical film. The apparent heights for the nanoshaved regions were determined from 100 nm × 100 nm squares in at least four locations, and the apparent heights for the Cu-ligated MHDA multilayer were determined from 500 nm× 500 nm squares in at least four locations adjacent to the nanoshaved regions.

Spectroscopic Ellipsometry

Spectroscopic ellipsometry measurements were acquired using a rotating compensator spectroscopic ellipsometer (Alpha-SE, J.A. Woollam Inc.) where 180 wavelengths between 380 - 900 nm were measured at a fixed 70° angle of incidence. The thicknesses of the SiO_2 layer on the Si substrate, the UTS monolayers, the UTS_{ox} monolayers, and the Cu-ligated MHDA multilayers were calculated using the CompleteEASE software package. The "Si with Native Oxide" model was used to determine the thickness of the SiO_2 layer on the Si substrate, and a "Cauchy" model was used to determine the thickness for the UTS monolayers, UTS_{ox} monolayers, and Cu-ligated MHDA multilayers using a refractive index value of $n = 1.5$.[29, 31, 33, 41] Measurements were collected on multiple regions across multiple Si substrates, UTS

monolayers, UTS_{ox} monolayers, and Cu-ligated MHDA multilayers. The average and standard deviation (average ± standard deviation) of the resulting calculated thicknesses were determined.

Scanning Electron Microscopy

Scanning electron microscope (SEM) images of the molecular-ruler samples were acquired using a TESCAN MIRA field-emission SEM. Images were taken at an accelerating voltage of 10.0 kV using the in-lens secondary electron detector at a working distance of approximately 5 mm.

RESULTS AND DISCUSSION

Cu-ligated MHDA Multilayer Growth on Si Substrates

Cu-ligated MHDA multilayers are commonly utilized to build up precise nanoscale lithographic resists to create tailored nanogaps. However, these Cu-ligated MHDA multilayers are typically assembled on Au substrates due to the selectivity of Au-thiol chemistry. In the present study, we demonstrate the growth of Cu-ligated MHDA multilayers on Si substrates. The morphology and structure of UTS monolayers, UTS_{ox} monolayers, and 15-layer Cu-ligated MHDA multilayers on Si substrates were investigated using contact-mode AFM and spectroscopic ellipsometry. Figure 2A shows a representative AFM topographic image of a 1 μm × 1 μm region of a UTS monolayer fabricated from a 5 mM bicyclohexyl solution of UTS, and Figure 2D shows a cursor profile across the UTS monolayer as indicated by the blue line in Figure 2A. The surface morphology and RMS roughness (0.2 ± 0.1 nm) of the SAM are consistent with densely-packed UTS SAMs, which is unsurprising given that similar deposition conditions have been previously shown to produce densely packed UTS monolayers.[9, 12, 42-43] Isolated protruding features are observed across the surface ranging in height from 1 nm to 5 nm. These features are consistent

with nonspecific absorption during the fabrication process. Figure 2B shows a representative AFM topographic image of a 1 μm × 1 μm region of a UTS_{ox} monolayer fabricated by oxidizing the terminal olefin groups of a preexisting UTS SAM, and Figure 2D shows a cursor profile across the UTS_{ox} monolayer as indicated by the green line in Figure 2B. Overall, the surface morphology and RMS roughness (0.5 ± 0.2 nm) are consistent with a densely-packed UTS SAM. Protruding features are observed on the UTS_{ox} SAMs with heights typically ranging from 1 nm to 8 nm, and in some instances features as tall as 15 nm are observed. An increase in the number, density, and size of isolated, protruding features is observed when compared to the UTS SAMs. This increase is attributed to an increase in nonspecific absorption due to the terminal carboxyl groups. It is important to note that there are variations in the number, density, and size of these protruding features from sample to sample. The thicknesses of the UTS SAMs (1.7 ± 0.1 nm) and UTS_{ox} SAMs (1.7 ± 0.1 nm) measured via spectroscopic ellipsometry are in agreement with the thickness of densely-packed UTS SAMs and indicate that organosilane SAMs remain after the oxidation of terminal olefin groups to carboxyl groups.

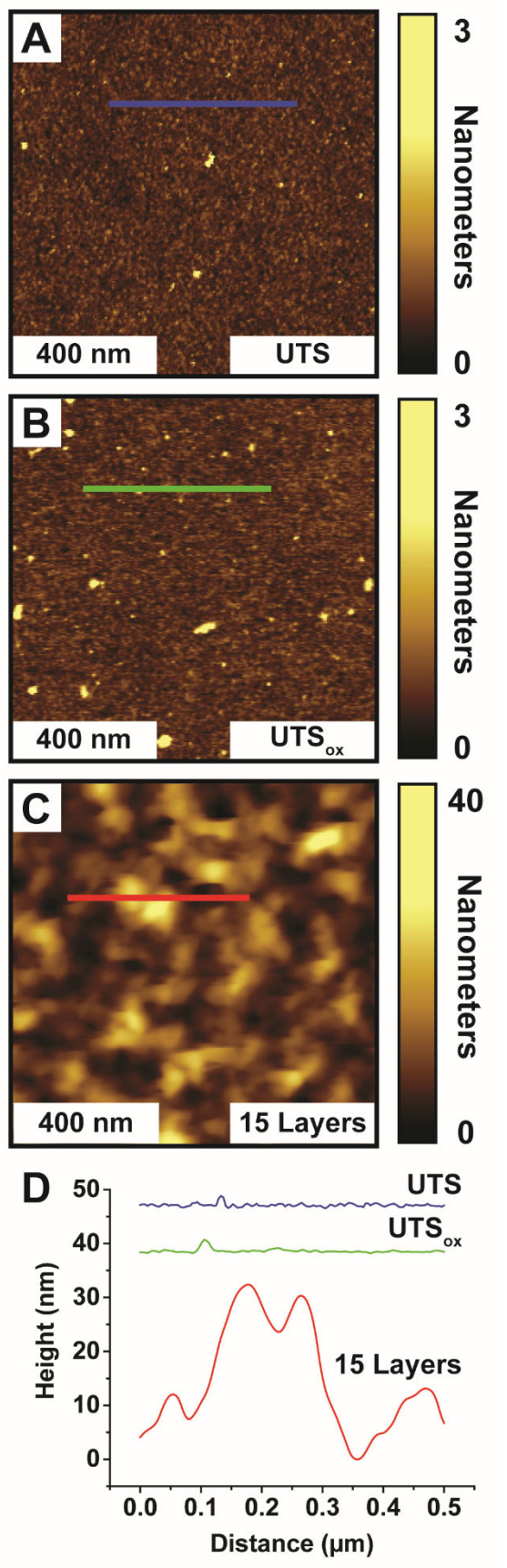
A
400 nm
UTS
3
Nanometers
0
B
400 nm
UTS$_{ox}$
3
Nanometers
0
C
400 nm
15 Layers
40
Nanometers
0
D
UTS
UTS$_{ox}$
15 Layers
Height (nm)
50
40
30
20
10
0
0.0
0.1
0.2
0.3
0.4
0.5
Distance (μm)

Figure 2. Comparison of the morphology and local structure of a UTS monolayer, UTS_{ox} monolayer, and 15-layer Cu-ligated Multilayer. Representative AFM images of (A) a UTS monolayer, (B) a UTS_{ox} monolayer, and (C) a 15-layer Cu-lagated MHDA multilayer fabricated on Si substrates. (D) Corresponding cursor profiles across the substrates as indicated in the AFM images. All AFM images were acquired under ambient conditions in contact mode with force setpoints of less than 1 nN.

Figure 2C displays a representative AFM topographic image of a 1 μm × 1 μm region of 15-layer Cu-ligated MHDA multilayer assembled onto a preexisting UTS_{ox} SAM, and Figure 2D shows a cursor profile across the multilayer as indicated by the red line in Figure 2C. The surface morphology, consisting of protruding and depressed regions across the surface, and a RMS roughness of 7.3 ± 0.4 nm are in stark contrast to the relatively smooth morphology of the UTS and UTS_{ox} monolayers. The thickness of the 15-layer Cu-ligated MHDA multilayer assembled onto of a preexisting UTS_{ox} SAM measured via spectroscopic ellipsometry is 37.4 ± 0.5 nm. It is important to note that this thickness represents both the preexisting UTS_{ox} SAM and the 15-layer Cu-ligated MHDA SAM. Using 1.7 nm as the thickness of the preexisting UTS_{ox} SAM, the thickness of the 15-layer Cu-ligated MHDA multilayer measures 35.7 nm. This multilayer thickness equates to 2.4 nm per iteration of $Cu(ClO_4)_2 \cdot 6H_2O$ and MHDA, which is in agreement with Cu-ligated MHDA multilayers assembled onto Au substrates.[29-30, 33, 41, 44] If UTS SAMs are subjected to iterative depositions of $Cu(ClO_4)_2 \cdot 6H_2O$ and MHDA, multilayer growth is not observed (data not shown), indicating that the oxidation of the UTS monolayer is critical to the assembly of Cu-ligated MHDA multilayers.

Nanoshaving of Cu-ligated MHDA Multilayers on Si Substrates

Figure 3A shows a representative AFM topographic image of a 1 μm × 1 μm region of a 15-layer Cu-ligated MHDA multilayer assembled on a preexisting UTS_{ox} SAM where nanoshaving has been performed; Figure 3B shows a cursor profile across the Cu-ligated MHDA multilayer and the nanoshaved regions as indicated by the red line in Figure 3A. Both imaging and nanoshaving were performed under ethanol. The depressed 400 nm × 600 nm rectangle corresponds to the nanoshaved region generated at a force setpoint of 80 nN. The morphology and features of the surrounding 15-layer Cu-ligated MHDA multilayer have been described above. The smooth morphology and RMS roughness of 0.3 ± 0.1 nm of the nanoshaved region indicate that the 15-layer Cu-ligated MHDA multilayer has been removed exposing the underlying UTS_{ox} monolayer. At a force setpoint of 80 nN, there is sufficient force to remove the Cu-ligated MHDA multilayer but insufficient force to remove the preexisting UTS_{ox} SAM. To remove organosilane SAMs, force setpoints on the order of μN are required.[26-28] The nanoshaved region appears 32.9 ± 1.9 nm lower than the 15-layer Cu-ligated MHDA multilayer. This depth is consistent with the spectroscopic ellipsometry measurements of 15-layer Cu-ligated MHDA multilayers assembled on preexisting UTS_{ox} SAMs as described above.

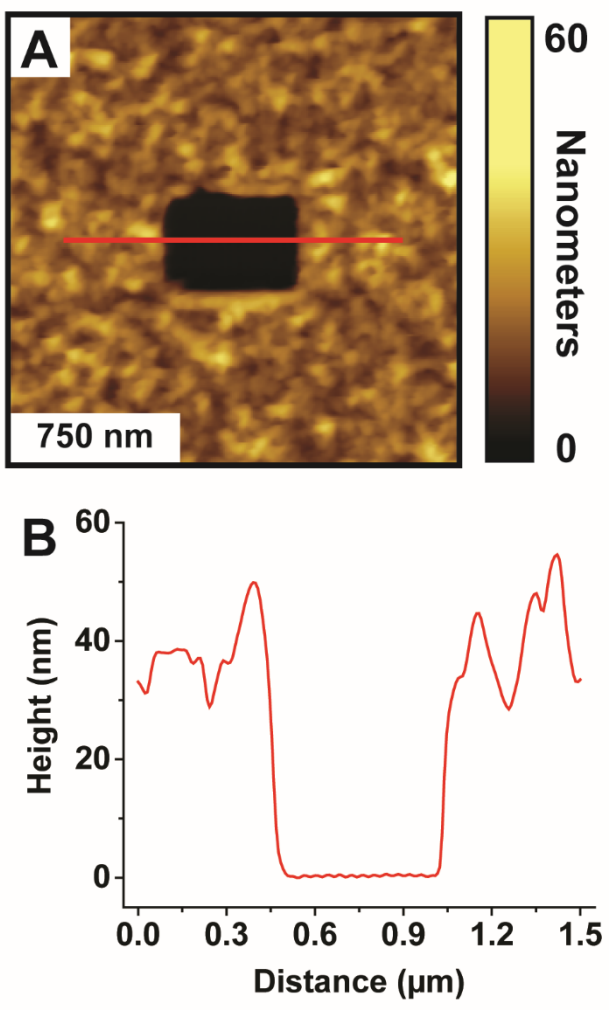

Figure 3. Morphology and local structure of a nanoshaved region of a 15-layer Cu-ligated multilayer. (A) A representative AFM image of a 15-layer Cu-ligated MHDA multilayer fabricated on a Si substrate with a nanoshaved region. (B) Corresponding cursor profiles across the preexisting multilayer and nanoshaved region indicated in the AFM image. The AFM image was acquired under ethanol in contact mode with a force setpoint of 1 nN.

Metal Nanopatterns Via Nanoshaving Cu-Ligated MHDA Multilayers on Si Substrates

To demonstrate the utility of Cu-ligated MHDA multilayers assembled on Si substrates, metal nanopatterns were generated using nanoshaving. Figure 4 shows the general approach. A Cu-

ligated MHDA multilayer assembled on a Si substrate is imaged at a low force setpoint (~1 nN) under ethanol to characterize the substrate and to locate an appropriate location for patterning. Using a high force setpoint (30-100 nN, depending on the sharpness of the AFM tip), the underlying preexisting UTS_{ox} SAM is exposed due to the tip-induced desorption of the Cu-ligated MHDA multilayer. Subsequently, the pattern region is imaged at a low force setpoint (~1 nN) to characterize the resulting chemical pattern. The substrate is removed from the liquid cell and placed into a thermal deposition system where metal is deposited across the entire substrate including the exposed UTS_{ox} region and the Cu-ligated MHDA multilayer regions. After metal deposition, a chemical lift-off removes the labile Cu-ligated MHDA multilayer, thus removing the metal masked by the Cu-ligated MHDA multilayer, yielding metal nanopatterns. The size and shape of the metal nanopatterns is defined by nanoshaving.

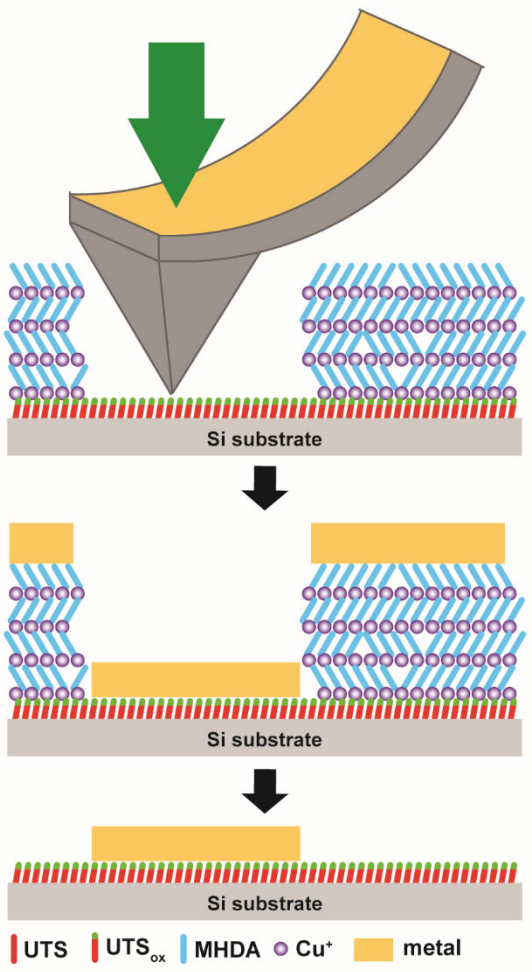

Figure 4. Key steps for the fabrication of metal nanopatterns on Si substrates via nanoshaving. Once a location for patterning is determined, to expose the preexisting UTS_{ox} SAM and to remove the Cu-ligated MHDA multilayer, a high force setpoint (30-100 nN) is applied during nanoshaving. After nanoshaving, metal is deposited across the entire substrate. Upon removal of the Cu-ligated multilayer and the metal on top of the multilayer via a chemical lift-off, a metal nanopattern is generated with the features of the nanoshaved region.

Figure 5A shows a representative AFM topographic image of a 1 μm × 1 μm region of a 15-layer Cu-ligated MHDA multilayer assembled on a preexisting UTS_{ox} SAM where nanoshaving has been performed. The depressed 550 nm × 550 nm square corresponds to the nanoshaved region generated at a force setpoint of 80 nN. Figure 5B shows a representative SEM image of the same region in Figure 5A after metal deposition and chemical liftoff. The higher-intensity regions correspond to the Au nanopattern, and the lower-intensity regions correspond to the Si substrate with the UTS_{ox} SAM. The features of the Au nanopattern are consistent with features of the nanoshaved region illustrating that the features created via nanoshaving can be translated to Au nanopatterns. Further, this demonstrates that Cu-ligated MHDA multilayers assembled onto preexisting UTS_{ox} monolayers can be used as molecular resists in a similar manner as Cu-ligated MHDA multilayers assembled onto Au substrates. To demonstrate the versatility of this approach, a more complex nanopattern was generated. Figure 5C shows a AFM topographic image of a 1.3 μm × 1.3 μm region of a 15-layer Cu-ligated MHDA multilayer assembled on a preexisting UTS_{ox} SAM where nanoshaving has been performed. The depressed 900 nm × 900 nm cross corresponds to the nanoshaved region generated at a force setpoint of 90 nN. Figure 5D shows a SEM image of the same region in Figure 5C after metal deposition and chemical-liftoff. Although there are a few defects in the Au nanopattern, the overall shape and complex features are translated from the nanoshaved pattern to the Au nanopattern.

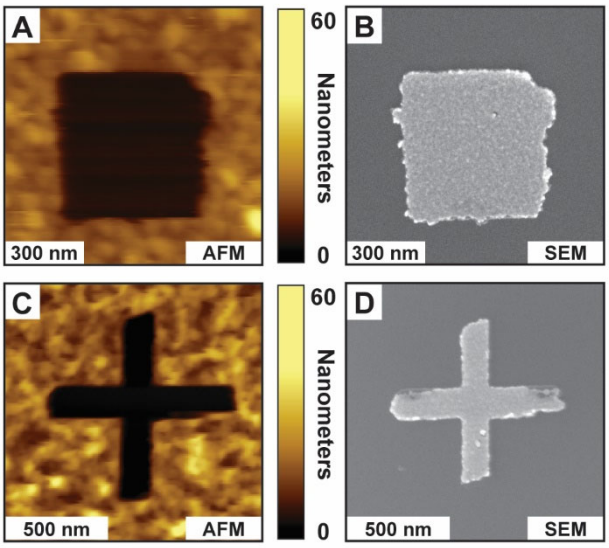

Figure 5. Comparison of nanoshaved regions and the resulting metal nanostructures. (A) A representative AFM image of a 15-layer Cu-ligated MHDA multilayer fabricated on a Si substrate with a nanoshaved square, and (B) corresponding SEM image of the resulting Au nanopattern. (C) A representative AFM image of a 15-layer Cu-ligated MHDA multilayer fabricated on a Si substrate with a nanoshaved cross, and (D) corresponding SEM image of the resulting Au nanopattern. The AFM images were acquired under ethanol in contact mode with force setpoints of less than 1 nN. The Au nanopatterns are 10 nm thick.

CONCLUSION

To overcome the challenges of nanoshaving organosilane SAMs, we have developed a process to assemble and pattern Cu-ligated MHDA multilayers on top of preexisting organosilane SAMs. Typically, Cu-ligated MHDA multilayers selectively assemble on Au substrates, relying on the Au- chemistries. However, by oxidizing the terminal olefin groups of a UTS SAM to carboxyl groups, Cu-ligated MHDA multilayers can be assembled onto organosilane SAMs, enabling multilayer growth on a wide variety of substrates. The interface between the UTS_{ox} SAM and

the Cu-ligated MHDA multilayer provides a natural low force breakpoint for nanoshaving. The resulting patterns can function as chemical resists for defining metal nanostructures. Compared to electron-beam lithography, this process enables the local area to be imaged before and in between patterning steps without affecting the chemical resist. This can be advantageous for achieving precise alignment between larger wafer-scale structures patterned by photolithography and smaller nanoscale features.

Such nanostructures have potential applications in nanoelectronics, molecular-scale junctions, and electrochemical sensors. In future work, we intend to explore the underlying mechanisms of Cu-ligated MHDA multilayer assembly on Si substrates and compare them to the assembly of Cu-ligated MHDA multilayers on Au substrates. Additionally, we plan to apply this strategy to other potential metal/ligand combinations.

ACKNOWLEDGEMENTS

This work was supported by the National Science Foundation (CMMI-1536528) and a UNF Academic Affairs Faculty Development Scholarship Grant. We thank Ms. Lauren Mann and Prof. Corey Causey for helpful and insightful discussions and the UNF Materials Science and Engineering Research Facility (MSERF) for the use of equipment.

REFERENCES

1. Onclin, S.; Ravoo, B. J.; Reinhoudt, D. N., Engineering Silicon Oxide Surfaces Using Self-Assembled Monolayers. *Angewandte Chemie-International Edition* **2005**, *44*, 6282-6304.

2. Aswal, D. K.; Lenfant, S.; Guerin, D.; Yakhmi, J. V.; Vuillaume, D., Self Assembled Monolayers on Silicon for Molecular Electronics. *Analytica Chimica Acta* **2006**, *568*, 84-108.

3. Pujari, S. P.; Scheres, L.; Marcelis, A. T. M.; Zuilhof, H., Covalent Surface Modification of Oxide Surfaces. *Angewandte Chemie-International Edition* **2014**, *53*, 6322-6356.

4. Ulman, A., Self-Assembled Monolayers of Alkyltrichiorosilanes: Building Blocks for Future Organic Materials. *Advanced Materials* **1990**, *2*, 537-582.

5. Gun, J.; Sagiv, J., On the Formation and Structure of Self-Assembling Monolayers. 3. Time of Formation, Solvent Retention, and Release. *Journal of Colloid and Interface Science* **1986**, *112*, 457-472.

6. Sagiv, J., Organized Monolayers by Adsorption. 1. Formation and Structure of Oleophobic Mixed Monolayers on Solid Surfaces. *Journal of the American Chemical Society* **1980**, *102*, 92-98.

7. Finklea, H. O.; Robinson, L. R.; Blackburn, A.; Richter, B.; Allara, D. L.; Bright, T., Formation of an Organized Monolayer by Solution Adsorption of Octadecyltrichlorosilane on Gold - Electrochemical Properties and Structural Characterization. *Langmuir* **1986**, *2*, 239-244.

8. Carson, G.; Granick, S., Self-Assembly of Octadecyltrichlorosilane Films on Mica. *Journal of Applied Polymer Science* **1989**, *37*, 2767-2772.

9. Wasserman, S. R.; Tao, Y. T.; Whitesides, G. M., Structure and Reactivity of Alkylsiloxane Monolayers Formed by Reaction of Alkyltrichlorosilanes on Silicon Substrates. *Langmuir* **1989**, *5*, 1074-1087.

10. Brandow, S. L.; Chen, M. S.; Aggarwal, R.; Dulcey, C. S.; Calvert, J. M.; Dressick, W. J., Fabrication of Patterned Amine Reactivity Templates Using 4-Chloromethylphenylsiloxane Self-Assembled Monolayer Films. *Langmuir* **1999**, *15*, 5429-5432.

11. Schreiber, F., Structure and Growth of Self-Assembling Monolayers. *Progress in Surface Science* **2000**, *65*, 151-256.

12. Wen, K.; Maoz, R.; Cohen, H.; Sagiv, J.; Gibaud, A.; Desert, A.; Ocko, B. M., Postassembly Chemical Modification of a Highly Ordered Organosilane Multilayer: New Insights into the Structure, Bonding, and Dynamics of Self-Assembling Silane Monolayers. *ACS Nano* **2008**, *2*, 579-599.

13. Dulcey, C. S.; Georger, J. H.; Krauthamer, V.; Stenger, D. A.; Fare, T. L.; Calvert, J. M., Deep Uv Photochemistry of Chemisorbed Monolayers - Patterned Coplanar Molecular Assemblies. *Science* **1991**, *252*, 551-554.

14. Smith, R. K.; Lewis, P. A.; Weiss, P. S., Patterning Self-Assembled Monolayers. *Progress in Surface Science* **2004**, *75*, 1-68.

15. Lercel, M. J.; Craighead, H. G.; Parikh, A. N.; Seshadri, K.; Allara, D. L., Sub-10 Nm Lithography with Self-Assembled Monolayers. *Applied Physics Letters* **1996**, *68*, 1504-1506.

16. Wang, D. W.; Thomas, S. G.; Wang, K. L.; Xia, Y. N.; Whitesides, G. M., Nanometer Scale Patterning and Pattern Transfer on Amorphous Si, Crystalline Si, and Sio2 Surfaces Using Self-Assembled Monolayers. *Applied Physics Letters* **1997**, *70*, 1593-1595.

17. Xia, Y. N.; Mrksich, M.; Kim, E.; Whitesides, G. M., Microcontact Printing of Octadecylsiloxane on the Surface of Silicon Dioxide and Its Application in Microfabrication. *Journal of the American Chemical Society* **1995**, *117*, 9576-9577.

18. Ivanisevic, A.; Mirkin, C. A., "Dip-Pen" Nanolithography on Semiconductor Surfaces. *Journal of the American Chemical Society* **2001**, *123*, 7887-7889.

19. Jung, H.; Kulkarni, R.; Collier, C. P., Dip-Pen Nanolithography of Reactive Alkoxysilanes on Glass. *Journal of the American Chemical Society* **2003**, *125*, 12096-12097.

20. Herzer, N.; Hoeppener, S.; Schubert, U. S., Fabrication of Patterned Silane Based Self-Assembled Monolayers by Photolithography and Surface Reactions on Silicon-Oxide Substrates. *Chemical Communications* **2010**, *46*, 5634-5652.

21. Li, J. R.; Lusker, K. L.; Yu, J. J.; Garno, J. C., Engineering the Spatial Selectivity of Surfaces at the Nanoscale Using Particle Lithography Combined with Vapor Deposition of Organosilanes. *ACS Nano* **2009**, *3*, 2023-2035.

22. Kooi, S. E.; Baker, L. A.; Sheehan, P. E.; Whitman, L. J., Dip-Pen Nanolithography of Chemical Templates on Silicon Oxide. *Advanced Materials* **2004**, *16*, 1013-1016.

23. Sulkanen, A. R.; Sung, J.; Robb, M. J.; Moore, J. S.; Sottos, N. R.; Liu, G. Y., Spatially Selective and Density-Controlled Activation of Interfacial Mechanophores. *Journal of the American Chemical Society* **2019**, *141*, 4080-4085.

24. Liu, G. Y.; Xu, S.; Qian, Y. L., Nanofabrication of Self-Assembled Monolayers Using Scanning Probe Lithography. *Accounts of Chemical Research* **2000**, *33*, 457-466.

25. Xu, S.; Liu, G. Y., Nanometer-Scale Fabrication by Simultaneous Nanoshaving and Molecular Self-Assembly. *Langmuir* **1997**, *13*, 127-129.

26. Lee, M. V., et al., Nanografting of Silanes on Silicon Dioxide with Applications to DNA Localization and Copper Electroless Deposition. *Chemistry of Materials* **2007**, *19*, 5052-5054.

27. Headrick, J. E.; Armstrong, M.; Cratty, J.; Hammond, S.; Sheriff, B. A.; Berrie, C. L., Nanoscale Patterning of Alkyl Monolayers on Silicon Using the Atomic Force Microscope. *Langmuir* **2005**, *21*, 4117-4122.

28. Xiao, X. D.; Liu, G. Y.; Charych, D. H.; Salmeron, M., Preparation, Structure, and Mechanical Stability of Alkylsilane Monolayers on Mica. *Langmuir* **1995**, *11*, 1600-1604.

29. Benson, A. S.; Elinski, M. B.; Ohnsorg, M. L.; Beaudoin, C. K.; Alexander, K. A.; Peaslee, G. F.; DeYoung, P. A.; Anderson, M. E., Metal-Organic Coordinated Multilayer Film Formation: Quantitative Analysis of Composition and Structure. *Thin Solid Films* **2015**, *590*, 103-110.

30. Drexler, C. I.; Moore, K. B., III; Causey, C. P.; Mullen, T. J., Atomic Force Microscopy Characterization and Lithography of Cu-Ligated Mercaptoalkanoic Acid "Molecular Ruler" Multilayers. *Langmuir* **2014**, *30*, 7447-7455.

31. Daniel, T. A.; Uppili, S.; McCarty, G.; Allara, D. L., Effects of Molecular Structure and Interfacial Ligation on the Precision of Cu-Bound Alpha,Omega-Mercaptoalkanoic Acid "Molecular Ruler" Stacks. *Langmuir* **2007**, *23*, 638-648.

32. Johnson, S.; Chan, J.; Evans, D.; Davies, A. G.; Waelti, C., Effect of Chain Length on the Assembly of Mercaptoalkanoic Acid Multilayer Films Ligated through Divalent Cu Ions. *Langmuir* **2011**, *27*, 1033-1037.

33. Evans, S. D.; Ulman, A.; Goppertberarducci, K. E.; Gerenser, L. J., Self-Assembled Multilayers of Omega-Mercaptoalkanoic Acids - Selective Ionic Interactions. *Journal of the American Chemical Society* **1991**, *113*, 5866-5868.

34. Hatzor, A.; Weiss, P. S., Molecular Rulers for Scaling Down Nanostructures. *Science* **2001**, *291*, 1019-1020.

35. Freeman, T. L.; Evans, S. D.; Ulman, A., Multilayers of Omega-Mercaptoalkanoic Acids Containing a Polar Aromatic Group - Characterization of Films. *Thin Solid Films* **1994**, *244*, 784-788.

36. Hutter, J. L.; Bechhoefer, J., Calibration of Atomic-Force Microscope Tips. *Review of Scientific Instruments* **1993**, *64*, 1868-1873.

37. Lo, Y. S.; Huefner, N. D.; Chan, W. S.; Dryden, P.; Hagenhoff, B.; Beebe, T. P., Organic and Inorganic Contamination on Commercial AFM Cantilevers. *Langmuir* **1999**, *15*, 6522-6526.

38. Necas, D.; Klapetek, P., Gwyddion: An Open-Source Software for Spm Data Analysis. *Central European Journal of Physics* **2012**, *10*, 181-188.

39. Shao, J.; Josephs, E. A.; Lee, C.; Lopez, A.; Ye, T., Electrochemical Etching of Gold within Nanoshaved Self-Assembled Monolayers. *Acs Nano* **2013**, *7*, 5421-5429.

40. Lee, C.; Josephs, E. A.; Shao, J.; Ye, T., Nanoscale Chemical Patterns on Gold Microplates. *Journal of Physical Chemistry C* **2012**, *116*, 17625-17632.

41. Patron, A. M.; Hooker, T. S.; Santavicca, D. F.; Causey, C. P.; Mullen, T. J., Expanding the Molecular-Ruler Process through Vapor Deposition of Hexadecanethiol. *Beilstein Journal of Nanotechnology* **2017**, *8*, 2339-2344.

42. Rye, R. R.; Nelson, G. C.; Dugger, M. T., Mechanistic Aspects of Alkylchlorosilane Coupling Reactions. *Langmuir* **1997**, *13*, 2965-2972.

43. Brownfield, A. L.; Causey, C. P.; Mullen, T. J., Effects of Surface Water on Organosilane Nanostructure Fabrication Using Particle Lithography. *Thin Solid Films* **2015**, *594*, 184-191.

44. Johnson, S.; Bronowska, A.; Chan, J.; Evans, D.; Davies, A. G.; Waelti, C., Redox-Induced Conformational Change in Mercaptoalkanoic Acid Multilayer Films. *Langmuir* **2012**, *28*, 6632-6637.

TABLE OF CONTENTS IMAGE